A Word from Alpine Tundra: Watch Out, Forests Are Invading!

Spatio-temporal Dynamics of Alpine Treeline Ecotones in the Western United States

Chenyang Wei & Adam M. Wilson, Ph.D.
Department of Geography, University at Buffalo, The State University of New York

Introduction

Where do trees survive in mountains? 1) Growing season ≥ ***3 months/94 days***. 2) Average air temperature during the growing season ≥ ***6.4 ℃***[2,5].

Alpine Treeline Ecotone (ATE) is: an unique and important ***ecological transition zone*** from subalpine ***forests*** to alpine ***tundra*** in global mountain environments (see the red rectangle in *Fig. 1*).

Why do we care about the ATE? 1) It's an ***essential habitat*** for numerous species (see *Fig. 2*). 2) It's relevant to many ***ecological functions*** such as carbon sequestration, nutrient and water cycling, snow retention, albedo and surface roughness, etc. 3) It is both a potential ***at-risk area*** and a powerful ***indicator*** of climate change[4] (see the red rectangles in *Fig. 3*).

ATE Characteristics

The ***study area*** (see the light gray area in *Fig. 4*) was determined based on a ***climate-based estimate*** of treeline elevation dataset[3,5].

Based on the NDVI and elevation data, we defined three ***ATE detection characteristics***[9]:

1) ***Abrupt spatial gradient in NDVI:*** NDVI typically decreases from montane to alpine zones (see "E1" in *Fig. 5* & "C1" in *Table 1*).
2) ***Intermediate NDVI:*** ATEs are typically characterized by intermediary NDVI values (see "E2" in *Fig. 5* & "C2" in *Table 1*). The Gaussian function was constructed based on the categorized NDVIs of the ***103 calibration pixels*** (see the orange dots in Fig. 4): a = 1, b = 0.44, and c = 0.06.
3) ***Spatial co-variation of elevation and NDVI:*** In ATEs, NDVI typically decreases as elevation increases (see "E3" in *Fig. 5* & component "C3" in *Table 1*).

ATE Detection Index

An ***ATE detection Index (ATEI)***[9] ranging from 0 to 1 was constructed by fitting a ***binomial logistic regression*** model of the three standardized components of the ***141 validation pixels*** (see the blue diamonds in *Fig. 4*). The coefficients of C1, C2, and C3 were 0.44, 0.58, and 0.56, respectively. The intercept was -1.47.

ATEI detection ***accuracy assessment***[9]: 1) 100-time repeated 10-fold ***cross-validation***: average overall accuracy = 0.713 (±0.111), average Kappa coefficient = 0.426 (±0.221). 2) An independent ***field-based*** ATE dataset[10] (see the yellow triangles in *Fig. 4*): Pearson's r = 0.98.

Transect Generation

Annual ATEI calculation from 1984 to 2018 (see *Fig. 6*) was based on: 1) annual max. NDVIs of ***LANDSAT***-5, 7, and 8[8], and 2) ***AW3D30*** elevation data[6,7].

Random transect generation (see *Fig. 7*): 1) Divide the study area into ***Thiessen polygons***. 2) Extract the ***steepest transect*** in each polygon. 3) Select transects with an average annual ***max. ATEI*** over 0.75 and a ***length*** between 500 m and 3 km. 4) Create a 30-m ***buffer*** of each selected transect.

Spatio-temporal Dynamics

ATE elevation trend analysis (see *Fig. 8*): 1) Extract the elevation of the pixel with the ***max. ATEI*** in each year within each transect. 2) Perform a ***robust linear regression*** between time and the extracted annual ATE elevation.

Estimated ATE elevation change from 1984 to 2018 in ***32,186 transects*** (see *Fig. 11*): 1) ***50.9%*** moving ***uphill*** (see the red area in *Fig. 10*) at ***6.25 m/decade***. 2) 22.9% moving downhill at -5.66 m/decade (see the blue area in *Fig. 10*). 3) 26.2 % no significant change (elevation trend between -1 and 1 m/decade, see the white area in *Fig. 10*).

Acknowledgements

This work was supported by NASA Headquarters under the NASA Earth and Space Science Fellowship Program - Grant "80NSSC18K1401".

Fig. 1. *An example of the Alpine Treeline Ecotone in Glacier National Park, MT.*

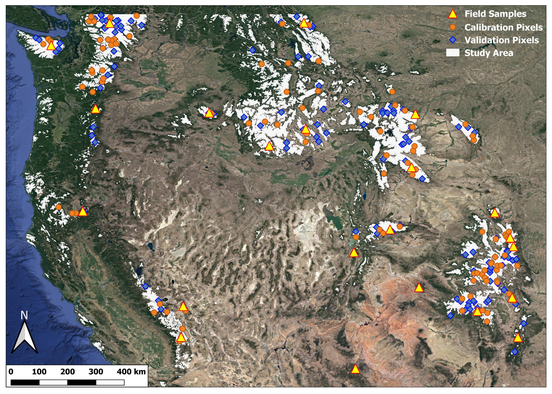

Fig. 4. *Geographic information of the study area and calibration/validation pixels in this study[9] (background image[1]). The yellow triangles represent the ground sampling sites located within the study area, which are from a published ATE research[10].*

(a) (b) (c)

Fig. 2. *Several species in ATEs: a) American pika (Ochotona princeps, source: Will Thompson photo, courtesy of USGS), b) Mountain goat (Oreamnos americanus, source: Darklich14 photo, courtesy of Wikimedia Commons), and c) a flag tree in Glacier National Park, MT.*

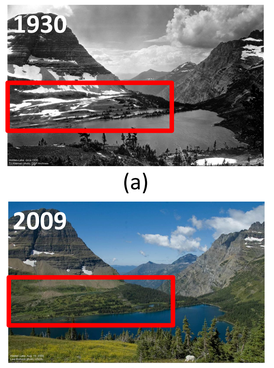

(a) (b)

Fig. 3. *Hidden Lake in Glacier National Park, MT in: a) 1930 (source: T.J. Hileman photo, courtesy of Glacier National Park Archives) and b) 2009 (source: Lisa McKeon photo, courtesy of USGS).*

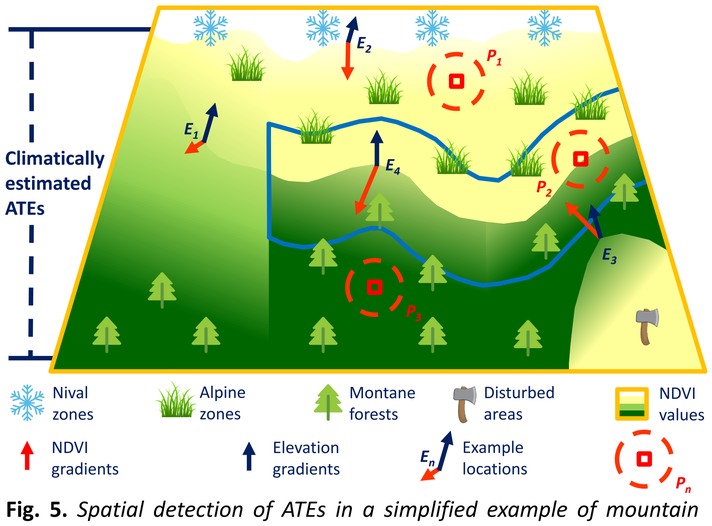

Fig. 5. *Spatial detection of ATEs in a simplified example of mountain environment[9].*

Table 1 *Defined characteristics of ATEs in this study[9]: 1) $\boldsymbol{C_1}$ quantifies the magnitude of NDVI gradient $\boldsymbol{\nabla f_{NDVI}}$ and depresses areas where NDVI varies gradually (see "E1" in Fig. 5). 2) $\boldsymbol{C_2}$ is a Gaussian function of f_{NDVI}, which depresses areas with very low or very high NDVI values, (see "E2" in Fig. 5). 3) $\boldsymbol{\nabla f_{Elv}}$ represents the elevational gradient[2]. $\boldsymbol{C_3}$ depresses areas where ∇f_{NDVI} and ∇f_{Elv} are in similar directions ($\theta < 90°$ or $\theta > 270°$, see "E3" in Fig. 5). Here, n is set to 10.*

No.	Algorithm	Component
C1	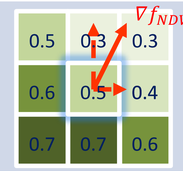	$\|\nabla f_{NDVI}\|$
C2	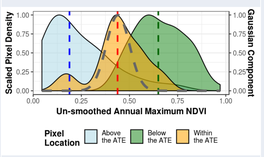	$ae^{\frac{(f_{NDVI}-b)^2}{2c^2}}$
C3	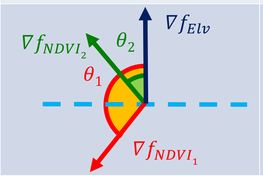	$\frac{(1-\cos\theta)^n}{2^n}$

$$ln\frac{ATEI}{1-ATEI} = \beta_0 + \sum_{i=1}^{3}\beta_i C_i \quad (i = 1,2,3)$$

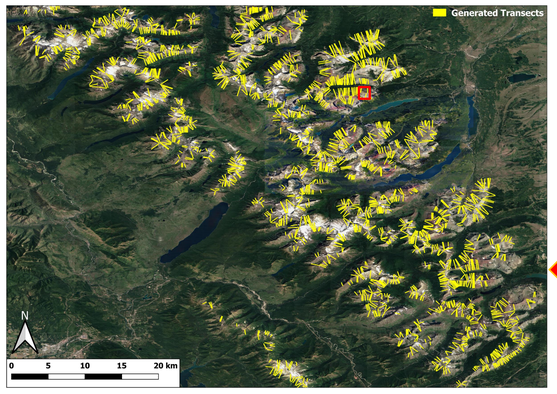

Fig. 7. *Selected transects in Glacier National Park, MT (background image[1]). The red rectangle shows the location of a transect example.*

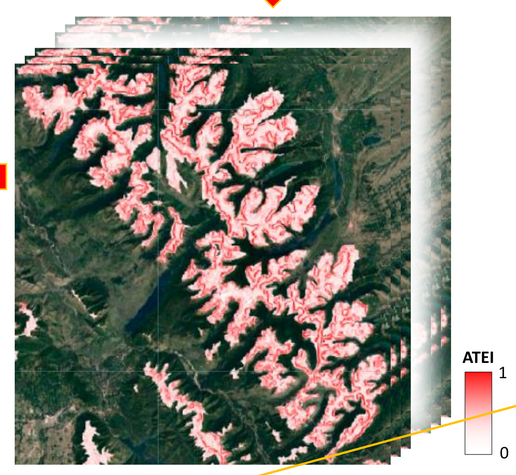

Fig. 6. *Annual ATEIs from 1984 to 2018 in Glacier National Park, MT (background image[1]).*

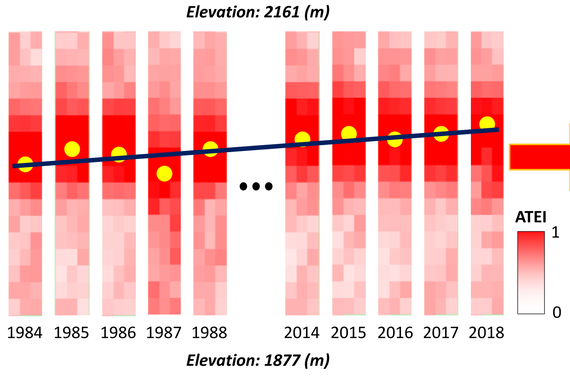

Fig. 8. *Annual ATEIs from 1984 to 2018 in a transect example (see the red rectangle in Fig. 7). The elevation of pixels within the transect varies from 1877 m a.s.l. to 2161 m a.s.l. The yellow dots indicate the pixel with the max. ATEI in each year. The dark blue line represents the trend line of the extracted annual ATE elevation.*

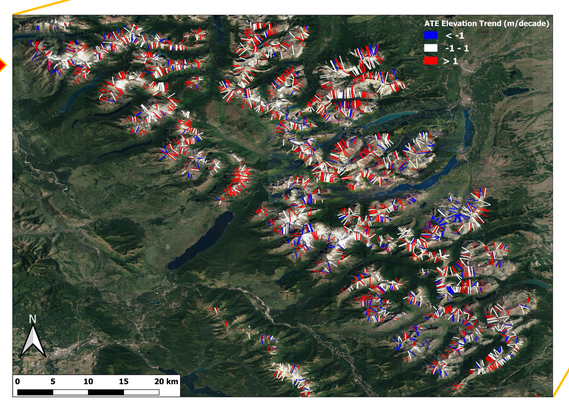

Fig. 9. *ATE elevation trends of all selected transects in Glacier National Park (background image[1]).*

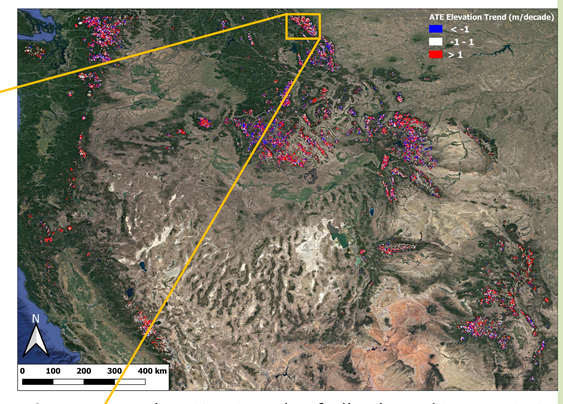

Fig. 10. *ATE elevation trends of all selected transects in the study area (background image[1]).*

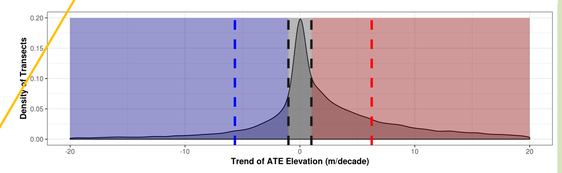

Fig. 11. *Distribution of the elevation trends of all selected transects in the study area.*

Contacts

Chenyang Wei
Department of Geography, University at Buffalo
Email: cwei5@buffalo.edu
Website: http://www.acsu.buffalo.edu/~cwei5/

Adam M. Wilson, Ph.D.
Department of Geography, University at Buffalo
Email: adamw@buffalo.edu
Website: http://adamwilson.us/

Google Earth Engine RStudio QGIS

Selected References

1. Google Maps, 2019. Satellite Imagery from the Google Maps [WWW Document]. Google Maps. URL http://www.maps.google.com (accessed 19).
2. Hoch, G., Körner, C., 2012. Global patterns of mobile carbon stores in trees at the high-elevation tree line. Glob. Ecol. Biogeogr. 21, 861–871.
3. Karger, D.N., Kessler, M., Conrad, O., Weigelt, P., Kreft, H., König, C., Zimmermann, N.E., 2019. Why tree lines are lower on islands—Climatic and biogeographic effects hold the answer. Glob. Ecol. Biogeogr. 28, 839–850.
4. Kennedy, R.E., Yang, Z., Gorelick, N., Braaten, J., Cavalcante, L., Cohen, W.B., & Healey, S., 2018. Implementation of the LandTrendr Algorithm on Google Earth Engine. Remote Sensing. 10, 691.
5. MacDonald, G., Kremenetski, K., & Beilman, D., 2008. Climate change and the northern Russian treeline zone. Philosophical Transactions of the Royal Society B: Biological Sciences, 363(1501), 2285-2299.
6. Paulsen, J., & Körner, C., 2014. A climate-based model to predict potential treeline position around the globe. Alpine Botany 124, 1–12.
7. Tadono, T., Ishida, H., Oda, F., Naito, S., Minakawa, K., Iwamoto, H., 2014. Precise global DEM generation by ALOS PRISM. ISPRS Annals of the Photogrammetry, Remote Sensing and Spatial Information Sciences 2, 71.
8. Takaku, J., Tadono, T., Tsutsui, K., 2014. GENERATION OF HIGH RESOLUTION GLOBAL DSM FROM ALOS PRISM. ISPRS Annals of Photogrammetry, Remote Sensing & Spatial Information Sciences 2.
9. USGS Earth Resources Observation & Science Center, 2019. Landsat Surface Reflectance Products of the Western United States from the United States Geological Survey Earth Resources Observation and Science Center [WWW Document]. URL (accessed 19).
10. Wei, C., Karger, D.N., & Wilson, A.M., in review. Spatial detection of alpine treeline ecotones in the western United States, Remote Sensing of Environment.
11. Weiss, D.J., Malanson, G.P., Walsh, S.J., 2015. Multiscale Relationships Between Alpine Treeline Elevation and Hypothesized Environmental Controls in the Western United States. Ann. Assoc. Am. Geogr. 105, 437–453.